

# Preferential Hydroxylation over Epoxidation Catalysis by a Horseradish Peroxidase Mutant: A Cytochrome P450 Mimic

Sam P. de Visser<sup>†</sup>

Manchester Interdisciplinary Biocenter and the School of Chemical Engineering and Analytical Science, The University of Manchester, 131 Princess Street, M1 7DN, Manchester, United Kingdom

Received: July 24, 2007

Density functional theory calculations are presented on the catalytic properties of a horseradish peroxidase mutant whereby the axial nitrogen atom is replaced by phosphorus. This mutant has never been studied experimentally and only one theoretical report on this system is known (de Visser, S. P. *J. Phys. Chem. B* 2006, 110, 20759–20761). Thus, a one-atom substitution in horseradish peroxidase changes the properties of the catalytic center of the enzyme to more cytochrome P450-type qualities. In particular, the phosphorus-substituted horseradish peroxidase mutant reacts with substrates via a unique reactivity pattern, whereby alkanes are regioselectively hydroxylated even in the presence of a double bond. Reaction barriers of propene epoxidation and hydroxylation are almost identical to ones observed for a cytochrome P450 catalyst and significantly higher than those obtained for a horseradish peroxidase catalyst. It is shown that the regioselectivity difference is entropy and thermally driven and that the electron-transfer processes that occur during the reaction mechanism follow cytochrome P450-type patterns in the hydroxylation reaction.

## Introduction

Cytochrome P450 enzymes (P450s) are a large group of heme enzymes involved in many bioprocesses in the body and catalyze, e.g., drug metabolism, the detoxification of compounds from the liver, and the biosynthesis of hormones.<sup>1</sup> Generally, the enzymes utilize molecular oxygen to form an oxoiron active species (compound I, CpdI) that reacts with substrates as a monooxygenase to give hydroxylated or epoxidized products. Extensive studies on P450 enzymes showed that these enzymes are able to regioselectively hydroxylate C–H bonds even in the presence of a C=C double bond.<sup>2</sup> This is an important quality of P450 enzymes, since generally C–H bonds are difficult to hydroxylate especially in the presence of a double bond. Thus, to exploit this for biotechnological purposes scientists have extensively searched for biomimetics that can reproduce this regioselectivity, based on the characteristic features of the P450 enzyme active site.<sup>3</sup> However, until now there is only one known example of a catalyst that indeed shows P450-type catalysis albeit it is a fairly sluggish oxidant and can only hydroxylate weak C–H bonds.<sup>4</sup> Therefore, characterizing catalysts that are able to hydroxylate C–H bonds in the presence of C=C double bonds is important.

A class of heme enzymes with an active site resembling the P450s is horseradish peroxidase (HRP). In these enzymes the heme is connected to the protein backbone via a histidine linkage rather than cysteinate.<sup>5</sup> A histidine ligand entices a different push effect on the iron-heme and thereby gives it different properties. As a result HRP binds molecular oxygen and converts it into hydrogen peroxide. By contrast, the P450s are monooxygenase enzymes that catalyze C–H hydroxylations, C=C epoxidations, sulfoxidations and *N*-dealkylations.<sup>1</sup> Extensive theoretical studies have characterized the active species of HRP and its reactivity patterns.<sup>6</sup> Thus, HRP CpdI is a triradicalar system with three unpaired electrons, two in  $\pi^*$  orbitals and a

third in a heme-type orbital labelled  $a_{2u}$ . These orbitals are either ferromagnetically coupled into a quartet spin state or antiferromagnetically coupled into a doublet spin state, which leads to multistate reactivity patterns.<sup>6c</sup> Recently, we presented calculations on an HRP CpdI mutant whereby the atom of the axial ligand that is bound to iron was replaced from nitrogen to phosphorus, CpdI(P).<sup>7</sup> The calculations showed that for CpdI-(P) this mutation changes the pull effect of the axial ligand to a push effect, and as a result it was predicted that it may have P450-type catalytic properties. This mutant, however, has never been experimentally studied; hence, the present calculations will predict its possible monooxygenation properties. Therefore, in order to test the predictions raised in ref 7, we present here results of calculations on the regioselective hydroxylation and epoxidation mechanisms of a phosphorus substituted HRP CpdI mutant. As will be shown, the mutant indeed gives P450-type catalysis with a preference of regioselective hydroxylation over epoxidation.

## Methods

All calculations were performed using established procedures in our group.<sup>8,9</sup> We used the unrestricted B3LYP hybrid density functional theory (DFT) in combination with a double- $\zeta$  quality LACVP basis set on iron and 6-31G on the rest of the atoms (basis set B1).<sup>10,11</sup> Full optimizations (without constraints) were performed in Jaguar 5.5 followed by an analytical frequency in Gaussian-03 with basis set B1.<sup>12,13</sup> All local minima had real frequencies only while the transition states are characterized by a single imaginary frequency for the correct mode. Subsequent, single-point calculations with a triple- $\zeta$  type LACV3P+ basis set on iron and 6-311+G\* on the rest of the atoms was performed (basis set B2).<sup>12</sup> All energies reported in this work correspond to UB3LYP/B2//UB3LYP/B1 energies with zero-point corrections obtained using the B1 basis set. Free energies were taken from the Gaussian frequency calculations and contain entropic and thermal corrections to the electronic energy at 298

<sup>†</sup> E-mail: sam.devisser@manchester.ac.uk.

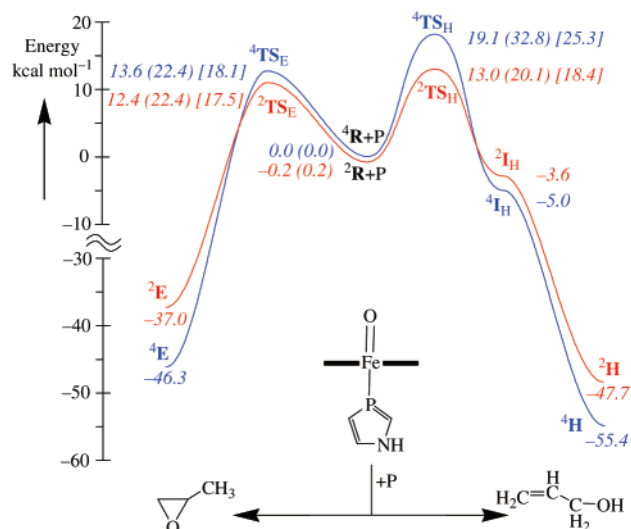


**Figure 1.** Potential energy profile for propene (P) epoxidation and hydroxylation by a phosphorus-substituted HRP mutant ( $^{4,2}\mathbf{R}$ ). All energies are in kcal mol $^{-1}$  relative to  $^4\mathbf{R}$  + propene. Free energies of activation ( $\Delta G^\ddagger$ ) are given in parenthesis and energies in a dielectric constant of  $\epsilon = 5.7$  in square brackets.

K. To estimate the effect of the environment on the reaction barriers we did single-point calculations in Jaguar using the self-consistent reaction field model with a dielectric constant of  $\epsilon = 5.7$  and a probe radius of 2.7 Å. All calculations were performed on the doublet and quartet spin state surfaces as identified with a superscript next to the label.

## Results and Discussion

Competitive C–H hydroxylation and C=C epoxidation of propene by CpdI(P) reactant ( $^{4,2}\mathbf{R}$ ) are shown in Figure 1. The epoxidation reaction is concerted via a C–O bond formation transition state ( $\mathbf{TS}_E$ ) directly leading to epoxide products ( $\mathbf{E}$ ). Calculations of epoxidation reactions catalyzed by P450 or HRP models gave stepwise reaction mechanisms via a radical intermediate.<sup>8</sup> Attempts here to locate a radical intermediate failed and converged back to the product complex. By contrast, the hydroxylation mechanism proceeds via an initial hydrogen abstraction barrier ( $\mathbf{TS}_H$ ) to form a hydroxo–iron complex with nearby allyl radical ( $\mathbf{I}_H$ ). The radical rebounds to the hydroxo group without barrier (see the Supporting Information) to form the propenol product complex ( $\mathbf{H}$ ). This mechanism is similar to the one obtained before for P450 and HRP models.<sup>8</sup>

The initial step in both reactions, i.e., via  $^{4,2}\mathbf{TS}_E$  or  $^{4,2}\mathbf{TS}_H$ , is rate determining, and three out of four transition states are within 1.2 kcal mol $^{-1}$  of each other at the  $\Delta E$  + ZPE level of theory. These barriers are within 1 kcal mol $^{-1}$  of the values obtained for P450 CpdI, where values of 12.8, 12.3, and 13.0 kcal mol $^{-1}$  were obtained for  $^{4}\mathbf{TS}_E$ ,  $^{2}\mathbf{TS}_E$ , and  $^{2}\mathbf{TS}_H$ , respectively, using the same methods and basis sets.<sup>8b</sup> As a consequence of the similar push effect of the axial ligand of CpdI(P) versus P450,<sup>7</sup> the barrier heights for epoxidation and hydroxylation are almost identical, whereas the barriers for HRP CpdI were several kilocalories per mole lower. Therefore, CpdI(P) shows P450-type activity in the reactions with substrates. In order to estimate the effect of the protein environment in an enzyme on the reaction barriers, we ran single point calculations in a dielectric constant of  $\epsilon = 5.7$ . These calculations, however, only have a minor effect on the ordering of the various transition states but increase the barrier heights by 4.5–6.2 kcal mol $^{-1}$  in energy. Consequently, the protein environment is not expected to

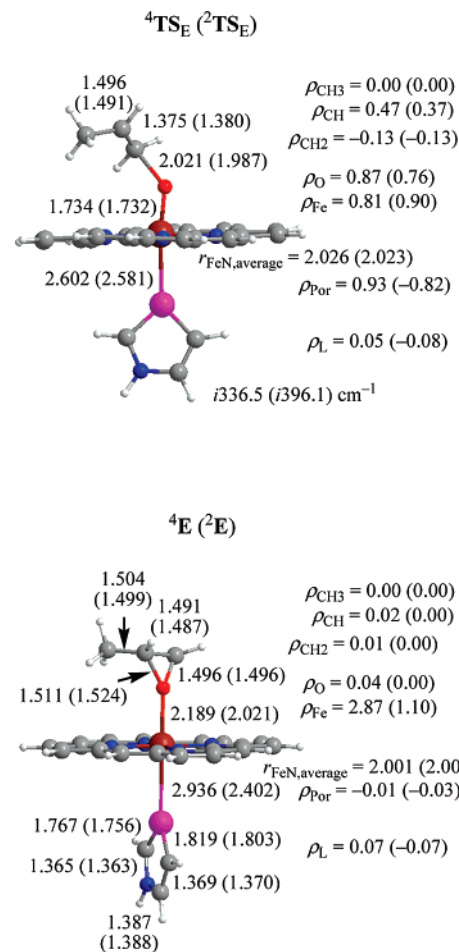


**Figure 2.** Optimized geometries of critical points along the epoxidation pathway:  $^{4,2}\mathbf{TS}_E$  (top) and  $^{4,2}\mathbf{E}$  (bottom) with bond lengths in angstroms. Also shown are group spin densities ( $\rho$ ) and the value of the imaginary frequency in cm $^{-1}$ .

influence the regioselectivity of hydroxylation over epoxidation in this reaction.

The free energies of activation give a slightly different picture for CpdI(P) whereby  $^{2}\mathbf{TS}_H$  is the lowest lying transition state by 2.3 kcal mol $^{-1}$  over  $^{4,2}\mathbf{TS}_E$ . Therefore, the regioselectivity preference of hydroxylation over epoxidation is determined by differences in the entropic and thermal contributions so that at 298 K hydroxylation is preferred. Recent studies of Takahashi et al.<sup>14</sup> on the regioselectivity of cyclohexene hydroxylation vs epoxidation by a synthetic oxoiron porphyrin catalyst also showed that the hydroxylation reaction is entropically controlled, whereas the epoxidation reaction is enthalpically controlled. Consequently, the barrier height ( $\Delta E$  + ZPE) and the regioselectivity preference of hydroxylation over epoxidation both implicate that the phosphorus-substituted HRP mutant mimics the catalytic properties of a P450 system. The free energy of activation barriers are close to the ones obtained experimentally for anthracene hydroxylation by a nonheme oxoiron system, so therefore the reaction between propene and the HRP mutant described here should be experimentally feasible.<sup>14</sup>

Figure 2 and 3 display the optimized geometries and group spin densities of the critical points along the reaction mechanism. Thus, in the epoxidation mechanism the substrate attacks the oxo group sideways indicating that an electron transfer from the substrate into the  $\pi^*_{xz}$  orbital takes place during this process. As a result, the FeO group loses spin density and the CH group of propene gains radical character. At the same time the Fe–O

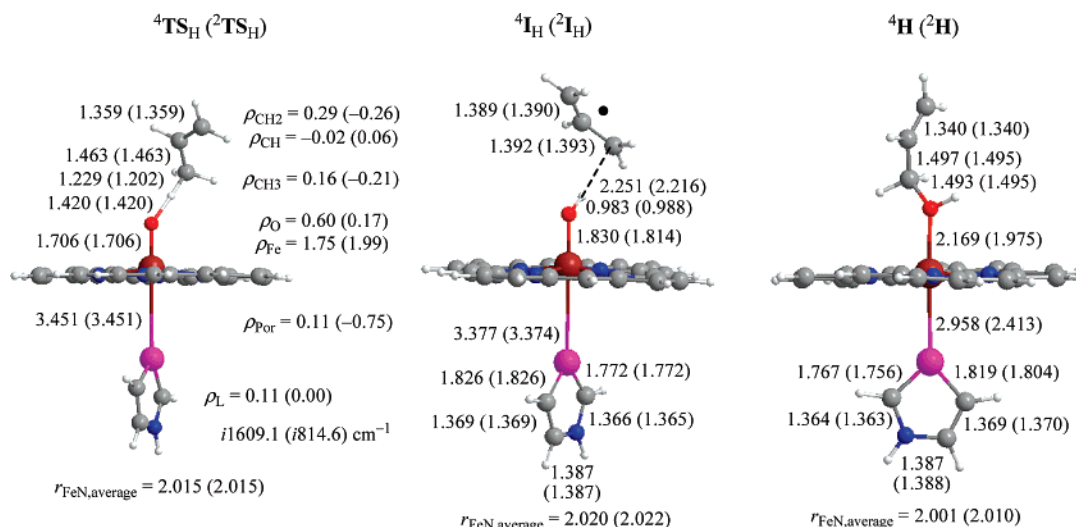


**Figure 3.** Optimized geometries of critical points along the hydroxylation pathway: <sup>4,2</sup>TS<sub>H</sub> (left), <sup>4,2</sup>I<sub>H</sub> (middle), and <sup>4,2</sup>H (right) with bond lengths in angstroms. Also shown are group spin densities (ρ) and the value of the imaginary frequency in cm<sup>−1</sup> of <sup>4,2</sup>TS<sub>H</sub>.

bond stretches to 1.734 (1.732) Å although the C–O bond is still rather long: 2.021 (1.987) Å for <sup>4</sup>TS<sub>E</sub> (<sup>2</sup>TS<sub>E</sub>) respectively. These distances are of the same order of magnitude as the ones obtained before by a P450 model CpdI.<sup>8b</sup> As soon as the C–O bond is relaxed to its ideal length, the epoxide ring closes to form the epoxide product complexes. Product formation results in weakening of the Fe–P and Fe–O bonds in <sup>4</sup>E, while the Fe–P distance shortens in <sup>2</sup>E. In the high-spin product complex one electron occupies the *σ*\*<sub>z2</sub> orbital that is antibonding along the O–Fe–P axis, hence these distances are elongated. Nevertheless, the spin density on the axial ligand remains small.

The hydroxylation transition states (Figure 3) show a more upright oriented structure indicating that an electron transfer takes place from the substrate into the *a*<sub>2u</sub> orbital rather than in *π*\*<sub>xz</sub> as was the case in the epoxidation mechanism. This electron transfer mechanism is confirmed by the group spin densities of <sup>4</sup>TS<sub>H</sub> which show a decrease of the porphyrin spin densities (to 0.11) and increase of radical character on the allyl rest group (0.43). The transition states occur early with short C–H and longer O–H distances: *r*<sub>C–H</sub> = 1.229 (1.202) and *r*<sub>O–H</sub> = 1.420 (1.420) for <sup>4</sup>TS<sub>H</sub> (<sup>2</sup>TS<sub>H</sub>), respectively. Although, geometrically <sup>4</sup>TS<sub>H</sub> and <sup>2</sup>TS<sub>H</sub> are very similar, their electronic properties differ distinctively. Namely, in the high-spin the spin density on the oxo group remains high (0.60), whereas in the low-spin it has dropped to 0.17. Simultaneously, the porphyrin is radical in the low-spin (−0.75), whereas it is only 0.11 in the high-spin. Nevertheless, both transition states lead to the same type of intermediate complex. Hydrogen abstraction considerably weakens the Fe–P bond since it lengthens these bonds to 3.451 Å in <sup>4,2</sup>TS<sub>H</sub>. This distance is shortened somewhat to 3.377 (3.374) Å in <sup>4,2</sup>I<sub>H</sub> (<sup>2</sup>I<sub>H</sub>) and decreases further to 2.958 (2.413) Å in <sup>4</sup>H (<sup>2</sup>H). Optimized geometries are similar to the ones obtained for P450 and HRP, except for the mentioned long Fe–P bond in the hydroxylation mechanism. Nevertheless, a frequency calculation confirms these structures to be stable minima. The Fe–P bond in the epoxidation is similar to the Fe–S bond in P450.<sup>8</sup>

The only difference between the studies presented here and previous work on P450 is regarding the group spin densities and therefore the electron distributions. The group spin densities on the oxo, iron, and porphyrin groups in <sup>4,2</sup>TS<sub>E</sub> are close to 1 implicating single occupation of *π*\*<sub>xz</sub>, *π*\*<sub>yz</sub>, and *a*<sub>2u</sub> molecular orbitals as is the case in the reactant.<sup>7</sup> These spin densities match the ones observed for <sup>2</sup>TS<sub>E</sub> of an HRP model, whereas for P450 the transition state had a more product-type electronic state. The

three lowest lying transition states all have a reactant-type electronic configuration, which shows that the electron-transfer processes occur late and only after passing the transition state. The spin densities for the reactant are ρ<sub>FeO</sub> = 2.02(2.05), ρ<sub>Por</sub> = 0.94(−1.03), and ρ<sub>L</sub> = 0.04(−0.07) for <sup>4</sup>R (<sup>2</sup>R), respectively.<sup>7</sup> Clearly, the spin density on the porphyrin group has decreased in <sup>2</sup>TS<sub>H</sub>, whereas it is roughly the same on the FeO group. Therefore, the hydrogen abstraction reaction is accomplished by electron transfer from the substrate into the singly occupied *a*<sub>2u</sub> (heme) orbital, whereby the metal remains in the Fe<sup>IV</sup> oxidation state. This is similar to P450 catalysis, where we showed that the reactions occur via Fe<sup>IV</sup> intermediates, whereas in HRP oxidations generally the intermediates have the metal in oxidation state Fe<sup>III</sup>.<sup>8</sup> The stability of these radical intermediates has been implicated as being responsible for side reactions leading to, e.g., suicidal complexes and cis–trans scrambling of epoxides.<sup>16</sup> Importantly, the absence of radical intermediates or radical intermediates with a short-lifetime will prevent the occurrence of significant amount of radical rearrangement products. Therefore, with phosphorus-substituted CpdI of HRP the amount of (unwanted) byproducts is expected to be very small.

## Conclusions

DFT studies on an HRP CpdI mutant with one nitrogen atom replaced by phosphorus gives a catalyst which follows P450-type catalysis whereby hydroxylation mechanisms are favored over epoxidation reactions. The reaction barriers obtained are similar to the ones calculated for a P450 CpdI model using the same methods, basis set and substrate. This regioselectivity is determined by favorable thermal and entropic corrections in the hydroxylation process. It is now up to synthetic biochemists to establish procedures to synthesize this exciting catalyst and test the above hypothesis.

**Acknowledgment.** The National Service of Computational Chemistry Software (NSCCS) is acknowledged for providing generous CPU time.

**Supporting Information Available:** Three tables with detailed group spin densities and charges, four figures with geometry scans and optimized geometries and Cartesian coordinates of all optimized geometries, as well as reference 13 in

full. This material is available free of charge via the Internet at <http://pubs.acs.org>.

## References and Notes

- (1) (a) Sono, M.; Roach, M. P.; Coulter, E. D.; Dawson, J. H. *Chem. Rev.* **1996**, *96*, 2841–2887. (b) Woggon, W.-D. *Top. Curr. Chem.* **1996**, *184*, 39–96. (c) Groves, J. T. *Proc. Natl. Acad. Sci. U.S.A.* **2003**, *100*, 3569–3574. (d) Ortiz de Montellano, P. R., Ed. *Cytochrome P450: Structure, Mechanism and Biochemistry*, 3rd ed.; Kluwer Academic/Plenum Publishers: New York, 2004.
- (2) Ruettinger, R. T.; Fulco, A. J. *J. Biol. Chem.* **1981**, *256*, 5728–5734.
- (3) (a) Costas, M.; Mehn, M. P.; Jensen, M. P.; Que, L., Jr. *Chem. Rev.* **2004**, *104*, 939–986. (b) Woggon, W.-D. *Acc. Chem. Res.* **2005**, *38*, 127–136.
- (4) Bukowski, M. R.; Koehntop, K. D.; Stubna, A.; Bominaar, E. L.; Halfen, J. A.; Münck, E.; Nam, W.; Que, L., Jr. *Science* **2005**, *310*, 1000–1002.
- (5) (a) Nicholls, P.; Fita, I.; Loewen, P. C. *Adv. Inorg. Chem.* **2000**, *51*, 51–106. (b) Veitch, N. G.; Smith, A. T. *Adv. Inorg. Chem.* **2000**, *51*, 107–162.
- (6) (a) Green, M. T. *J. Am. Chem. Soc.* **2000**, *122*, 9495–9499. (b) de Visser, S. P.; Shaik, S.; Sharma, P. K.; Kumar, D.; Thiel, W. *J. Am. Chem. Soc.* **2003**, *125*, 15779–15788. (c) Derat, E.; Shaik, S. *J. Am. Chem. Soc.* **2006**, *128*, 8185–8198.
- (7) de Visser, S. P. *J. Phys. Chem. B* **2006**, *110*, 20759–20761.
- (8) (a) de Visser, S. P.; Ogliaro, F.; Sharma, P. K.; Shaik, S. *Angew. Chem., Int. Ed.* **2002**, *41*, 1947–1951. (b) de Visser, S. P.; Ogliaro, F.; Sharma, P. K.; Shaik, S. *J. Am. Chem. Soc.* **2002**, *124*, 11809–11826. (c) Kumar, D.; de Visser, S. P.; Sharma, P. K.; Derat, E.; Shaik, S. *J. Biol. Inorg. Chem.* **2005**, *10*, 181–189.
- (9) (a) de Visser, S. P. *J. Am. Chem. Soc.* **2006**, *128*, 9813–9824. (b) de Visser, S. P. *J. Am. Chem. Soc.* **2006**, *128*, 15809–15818.
- (10) (a) Becke, A. D. *J. Chem. Phys.* **1993**, *98*, 5648–5652. (b) Lee, C.; Yang, W.; Parr, R. G. *Phys. Rev. B* **1988**, *37*, 785–789.
- (11) Hay, P. J.; Wadt, W. R. *J. Chem. Phys.* **1985**, *82*, 299–310.
- (12) *Jaguar 5.5*; Schrödinger, LLC: Portland, OR, 2003.
- (13) Frisch, M. J.; et al. *Gaussian-03*, revision C.01; Gaussian, Inc.: Wallingford, CT, 2004.
- (14) Takahashi, A.; Kurahashi, T.; Fujii, H. *Inorg. Chem.* **2007**, *46*, 6227–6229.
- (15) de Visser, S. P.; Oh, K.; Han, A.-R.; Nam, W. *Inorg. Chem.* **2007**, *46*, 4632–4641.
- (16) de Visser, S. P.; Ogliaro, F.; Shaik, S. *Angew. Chem., Int. Ed.* **2001**, *40*, 2871–2874.